THE GROWTH OF MULTI-SITE FATIGUE DAMAGE IN FUSELAGE LAP JOINTS

Robert S. Piascik
NASA Langley Research Center
Hampton, VA, 23681 USA.
Tel: (757) 864-3483
Fax: (757) 864-8911
E-Mail: r.s.piascik@larc.nasa.gov

Scott. A. Willard
Lockheed Engineering and Sciences Co.
Hampton, VA, 23681 USA.

ABSTRACT

Destructive examinations were performed to document the progression of multi-site damage (MSD) in three lap joint panels that were removed from a full scale fuselage test article that was tested to 60,000 full pressurization cycles. Similar fatigue crack growth characteristics were observed for small cracks (50 μm to 10mm) emanating from counter bore rivets, straight shank rivets, and 100° counter sink rivets. Good correlation of the fatigue crack growth data base obtained in this study and FASTRAN Code predictions show that the growth of MSD in the fuselage lap joint structure can be predicted by fracture mechanics based methods.

1. INTRODUCTION

To predict the growth of multi-site fatigue damage in fuselage structures, it is essential to thoroughly understand the processes that govern fatigue crack initiation and growth. The objective of this research is to:

- develop a fatigue crack database that completely describes the initiation and growth of small cracks in the riveted lap joint fuselage structure,
- provide a basis for comparing the crack growth behavior simulated in laboratory test specimens to the behavior in actual aircraft components, and
- serve as a benchmark to verify fatigue crack growth analytical methodology.

This research will assist in developing engineering tools that predict the onset of widespread fatigue damage (WFD), assist in setting damage inspection intervals, and quantify non-detectable damage prior to repair.

Multi-site damage (MSD) is defined as the simultaneous presence of multiple fatigue cracks in the same structural element (1). For MSD to occur, it is likely that the same damage process takes place at multiple locations within the same structural element. For the lap joint, similar damage processes occur at multiple rivet locations along the same rivet row. The thorough understanding of the MSD processes is required to develop deterministic methods for predicting the onset and growth of fatigue cracks. From this study, the detailed characterization of crack initiation sites at rivet holes will assist in the development of probabilistic and/or equivalent initial flaw size (EIFS) methods used to model crack nucleation. Fractographic analysis is used to catalog crack front morphologies that are essential for developing crack-tip stress intensity factor expressions for MSD. In addition, a comprehensive database is developed to validate fatigue crack growth predictions.

2. RESULTS AND DISCUSSION

A comprehensive destructive examination was conducted on three lap joint panels (panels 1, 3, and 6) removed from a full-scale test article pressurized to 60,000 cycles (2-4). During full-scale fatigue testing, visible outer skin cracks were noted in lap joints located at three isolated regions of the test article depicted in Figure 1. The regions that exhibited cracks were removed for detailed fractographic examinations. Panel 1 was removed from the bottom region of the test article and panels 3 and 6 were removed from two different locations along the side of the test article. The destructive examinations summarized herein describe the initiation and growth characteristics of small cracks emanating from counter bore, straight shank, and 100° countersink riveted lap joints. A brief description of each panel is summarized in Table 1. A detailed description is provided in references 2-4. These data are compared to independent small crack laboratory test results and are used to benchmark MSD crack growth predictions.

TABLE 1 PANEL DESCRIPTION

Panel #	No. of Rivet Rows	No. of Bays*	Rivet Type	Comments
1		6	Counter Bore	Visible cracks in bays 2-6
3	3	5	Straight Shank & 100° Countersink	Visible cracks in bay 2
6	4	5	Counter Bore	Visible cracks in bays 1-3, & 5

* A bay is the portion of lap joint (≈ 1.5 ft. long) located between adjacent tear straps.

2.1 DESTRUCTIVE EXAMINATIONS

Table 2 summarizes the results of the destructive examinations (2-4). A total of 419 rivet holes were examined for the presence of fatigue cracks by performing detailed optical and scanning electron microscopy (SEM) on approximately 2500 specimens. The precise location of the crack relative to the structure was documented and all fracture surfaces were characterized to document the site of crack initiation, crack front morphology, and fracture surface marker band details (discussed later). The examinations revealed that 45%, 77%, and 33% of the rivet holes examined in panels 1, 3, and 6, respectively, contained fatigue cracks.

TABLE 2 DESTRUCTUVE EXAMINATION SUMMARY

	Panel #1	Panel #3	Panel #6
No. of Bays Examined	3*	3	½
No. of Rivet Holes Examined	256	133	30
No. of Rivet Holes with Cracks	126	103	10
Percentage of Holes with Cracks	45%	77%	33%
No. of Fatigue Cracks Found	188	136	16

* Tear strap regions were examined in panel #1.

2.2 FATIGUE CRACK INITIATION

MSD in the fuselage lap joint is a likely result of cracks nucleating from fretting damage and regions of high stress concentration. The majority of fatigue cracks found in the counter bore riveted lap joint initiated along the faying surface (the interface between the outer and inner skins) of the outer skin

shown in Figure 2. Here, clad layer fretting along the faying surface was caused by repeated relative movement of the inner and outer skin in a highly localized contact area around the rivet hole. A black aluminum oxide on the faying surface marked the fretted region that containing debris and microcracks shown in Figures 2c and 2d. From this highly localized damaged region, fatigue cracks grew initially in a near semicircular manner (Figure 2a). As fatigue crack length increased, the crack front became elliptical in shape (Figure 2b). Many outer skin fatigue cracks propagated to a length of nearly two skin thicknesses prior to breaking through the outboard surface of the outer skin. A likely cause for subsurface cracking is lap joint bending loads and/or compressive residual stress produced from rivet head expansion into the counter bore region of the rivet hole. Figure 3 shows a typical region of crack initiation for the straight shank rivet. Figure 3a shows the fretting damage area (region A in Figure 3c) along the inboard surface of the straight shank hole. Figure 3c shows the fatigue crack and rivet hole region at an oblique angle. The micrograph shown in Figure 3b reveals an abraded surface containing microcracks similar to that observed in Figure 2d. Examination of the rivet shank mating surface (directly opposite of the abraded hole surface) revealed a black aluminum oxide region characteristic of fretting. The elliptical crack front shape shown in Figure 3d suggests the presence of lap joint bending loads (similar to that observed for the counter bore rivet (Figure 2)). The three examples shown in Figure 4a are typical examples of cracking observed in the 100°-countersink lap joint. Inboard corner cracks and shank/countersink corner cracks are located in regions of high stress concentration. These regions also exhibited some evidence of rivet/hole contact suggesting that fretting may have contributed to crack initiation. The third small fatigue crack shown in Figure 4a is located along the rivet hole surface in the rivet shank region; here, fretting is a likely cause for crack initiation. The dashed lines in Figures 4a and 4b mark the crack fronts and show that the small cracks in Figure 4a are circular in shape and at longer crack lengths, shown in Figure 4b, the crack front is somewhat circular in shape.

2.3 FATIGUE CRACK GROWTH DATA BASE

The growth rate of fatigue cracks 50 μm to 10 mm in length contained in panels 1, 3, and 6 was determined by performing detailed fractographic examinations (2-4). The examinations quantitatively determined the rate of crack propagation by tracking the progression of the fatigue crack front determined by the precise location of crack surface marker bands. During full-scale pressure testing, the pressure load was altered to form coded markings (marker bands) on fatigue crack surfaces contained in the lap joint. Figure 5 is an SEM micrograph showing an example of a fatigue crack surface marker band. Here, a six band code is used to mark the exact location of the crack front for a fatigue crack in panel 1 at 30,000 pressure cycles. Knowing the exact location the crack front at a known load cycle, a comprehensive fatigue crack growth database was developed.

The data shown in Figures 6 and 7 show that upper rivet row fatigue cracks contained in panels 1, 3, and 6 exhibit identical crack growth characteristics. Figures 6a, 6b, and 6c are plots showing marker band based fatigue crack growth rate (da/dN) data for cracks propagating from counter bore rivet holes, straight shank rivet holes, and 100° counter sink rivet holes, respectively. A comparison of the linear regression analysis (dashed and dotted lines) in Figures 6a and 6b reveal that:

- all counter bore cracks in panel 1 (bays 2, 3, and 4) exhibit the same crack growth characteristics, and
- all straight shank cracks in Panel 3 (bays 1 and 2) and Panel 6 (bay 4) exhibit the same crack growth characteristics.

A minimal amount of data from 100° counter sink rivet holes is shown in Figure 6c for panel 3 (bay 3). The excellent agreement of 100° counter sink crack growth rate data with the linear regression

analysis from Figures 6a and 6b (dashed line in Figure 6c) suggests that all fatigue cracks contained in the three different rivet configurations exhibit similar crack growth rate characteristics. A summary of all marker band based da/dN data is presented in Figure 7. This plot reveals that fatigue crack growth in riveted lap joint fuselage structure is well behaved; here, no appreciable difference is observed for data obtained from three rivet configurations, seven lap joint bays, and three different fuselage locations. The quantitative data in Figure 7 strongly suggest that the fatigue crack growth behavior of lap joint cracks ranging in size from 50 μm to 10 mm is deterministic and predictable.

Quantifying the fatigue crack growth rates for cracks of length less than 100 μm is problematic. Within the microstructural small crack regime (crack lengths < 50 to 100 μm), marker band analysis becomes extremely difficult and little data was obtained from the riveted structure. To estimate the growth rate behavior of microstructural small fatigue cracks in the lap joint, laboratory test results were used. The local stress at the rivet hole was estimated using the same procedure used for previous predictions of fatigue crack growth in panel 1 (5). Here, a neat pin (rivet) was assumed and a local stress of 143 MPa was estimated from the following parameters: S_{remote} = 90 MPa (remote stress in based on test article operational pressure) (6), 29% of the load is carried by the upper rivet in a four rivet row lap joint, and bending is $S_{bending} = \gamma S_{remote}$ where $\gamma = 0.5$ (7,8). A large body of small crack growth data for aluminum alloy 2024-T3 was generated by a "round robin program" conducted by thirteen laboratories (9). Each laboratory used a single edge (blunt) notch specimen and a replica technique for monitoring the growth of surface and corner fatigue cracks propagating from the blunt notch tested at a local stress level of 145 MPa. Because the small crack growth data were generated at a local stress level similar to the estimated local stress in the lap joint rivet hole, a comparison of laboratory and lap joint fatigue crack growth characteristics can be made. The laboratory microstructural small crack data are compared to the marker band data from panels 1, 3, and 6 in Figure 8 with the general assumption that local stresses due to rivet expansion are second order (neat pin assumption). The results shown in Figure 8 reveal the typical large scatter in microstructural small crack growth data; here, wide variations in small crack growth data are a result of crack front / microstructure interactions (10). A comparison of the linear regression analysis for the lap splice panel data (thick line) with the laboratory small crack data (thin line) suggests a strong correlation between the two data sets. Assuming that rivet fit-up effects are second order, the combined data base shown in Figure 8 represents the fatigue crack growth characteristics for riveted lap joint fuselage structure for crack lengths ranging from the microstructural small regime to 10 mm.

2.4 FATIGUE CRACK GROWTH PREDICTION

Fatigue crack growth predictions made by FASTRAN, a plasticity-induced crack closure based code, are in excellent agreement with lap joint marker band derived crack growth data. Compared in Figure 9 are the fatigue crack growth data and linear regression analysis results (dashed and dotted lines) from the destructive examinations conducted on panels 1, 3, and 6 and the results of two FRASTRAN predictions (5). The combined remote and bending load prediction is in good agreement with the panel data for crack lengths of less than one skin thickness and nearly duplicate the linear regression results. The prediction, using only remote stress, under predicts crack growth rates in the short crack regime (<1 mm). The abrupt transition in the predicted results at crack lengths equal to the skin thickness is due to the change in the crack-tip stress intensity factor expression as the subsurface crack emerges through the outer skin thickness. The results shown in Figure 9 demonstrate that fracture mechanics based analytical methods accurately predict the fatigue crack growth rate behavior in lap joints from distinctly different fuselage locations and containing different rivet configurations (counter bore, straight shank, and 100° counter sink rivets).

The FASTRAN prediction using remote and bending lap joint loads is compared to the marker band based crack length versus load cycle data in Figure 10. Two distinct populations are noted in Figure 10, the open circle data are those cracks that initiated first and grew to longer lengths and the solid data points are cracks that initiated later in life. The straight hole / neat pin prediction shown in Figure 10 assumes an EIFS of 50 μm. The EIFS was based on early destructive examination results suggesting that faying surface fretting in the clad layer (nominal thickness of 50 μm) initiated most upper rivet row lap splice fatigue cracks (2). These assumed parameters resulted in predictions that are in good agreement with most of the counter bore riveted lap joint data (solid data points) in Figure 10a and straight bore riveted lap joint data (solid data points) in Figure 10b. A twenty-percent error is observed between the predicted crack length and the measured crack length (open data points) at 60,000 pressure cycles. It is speculated that the life prediction did not approximate crack (a versus N) behavior (open data points) because fit up stresses may have been significant for those cracks that initiated earlier in life. As these first fatigue cracks grew, fit up forces at neighbor rivet locations decreased. More rigorous predictions are required; they should include, (1) accurate crack-tip stress intensity expressions for observed crack configurations, (2) accurate local stress concentration factor for the rivet hole configuration, (3) understanding of lap splice rivet hole local stress relaxation as a function of fatigue life, and (4) an appropriate EIFS for each fatigue crack initiation type.

SUMMARY

This research has established a comprehensive data-base that fully characterizes fuselage riveted lap joint multi-site fatigue damage. After 60,000 pressure cycles, the fuselage exhibits isolated regions of lap joint MSD that is characterized by small fatigue cracks contained in 50 to 80 percent of the rivet holes. Crack initiation is linked to mating surface fretting damage and regions of high stress concentration. The upper rivet row is most prone to subsurface outer skin crack growth; here, cracks can grow to two thicknesses in crack length before penetrating the outer skin outboard surface. No appreciable difference in fatigue crack growth characteristics was observed for cracks emanating from three rivet configurations, seven lap joint bays, and three different fuselage locations. These quantitative data strongly suggest that the fatigue crack growth behavior of lap joint cracks ranging in size from 50 μm to 10 mm is deterministic and predictable. Excellent correlation between marker band based lap joint fatigue crack growth rates and laboratory data suggest that microstructural small crack data can be used to verify predictions. FASTRAN code predictions of fatigue crack growth correlate with the destructive examination data base, thus showing that fracture mechanics based methods predict the growth of multi-site fatigue damage in the lap joint.

ACKNOWLEDGEMENT

The authors wish to gratefully acknowledge Mr. Michael L. Gruber and Ms. Anastasia Arseniev of the Boeing Co. for their technical guidance.

REFERENCES

1. Swift, T., "Widespread Fatigue Damage Monitoring – Issues and Concerns", Proc. of Intn'l. Symposium on Advanced Structural Integrity Methods for Airframe Durability and Damage Tolerance, Edited by C.E. Harris, NASA Conf. Pub. 3274, Hampton, VA, 1994, pp. 829-870.

2. Piascik, R.S. and Willard, S.A., "The Characterization of Fatigue Damage in the Fuselage Riveted Lap Splice Joint", NASA/TP-97-206257, National Aeronautics and Space Administration, Washington, D.C., 1997.
3. Piascik, R.S., Panel #3 Destructive Examination Results, to be published.
4. Piascik, R.S., Panel #6 Destructive Examination Results, to be published.
5. Piascik, R.S. and Willard, S.A., "The Characterization of Multi-Site Fatigue Damage in the Fuselage Riveted Lap Splice Joint", ICAF 97 Fatigue in New and Aging Aircraft, EMAS Publishing, 339 Halesowen Rd., Cradley Heath, West Midlands, UK, 1997, pp.93-114.
6. Gruber, M.L., Mazur, C.J., Wilkins, K.E., and Worden, R.E., "Investigation of Fuselage Structure Subjected to Widespread Fatigue Damage", DOT/FAA/Ar-95/47, National Technical Information Service, Springfield, VA, Feb. 1996.
7. Hartman, A. and Schijve, J., "The Effect of Secondary Bending on the Fatigue Strength of 2024-T3 Alclad Riveted Joints", NLR TR 69116U, Nat. Aerospace Lab. of the Netherlands, 1972.
8. Schijve, J., "Some Elementary Calculations on Secondary Bending in Simple Lap Joints", NLR TR 72036, Nat. Aerospace Lab. of the Netherlands, 1972.
9. Newman, J.C., Jr., and Edwards, P.R., "Short-Crack Growth Behavior in an Aluminum Alloy – An AGARD Cooperative Test Programme", AGARD Report No. 732, 1988.
10. Small Fatigue Cracks, Edited by R.O. Ritchie and J. Lankford, TMS-AIME, Warrendale, PA., 1986.

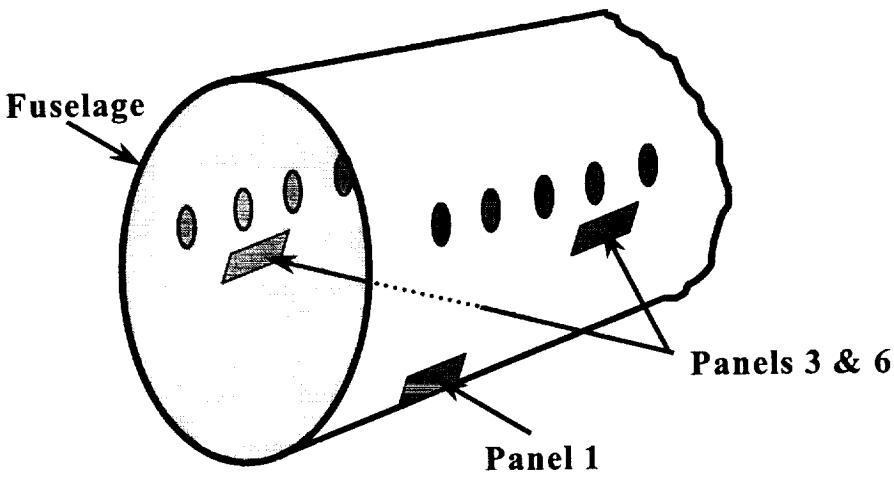

Figure 1. Schematic showing the location of the tear down panels.

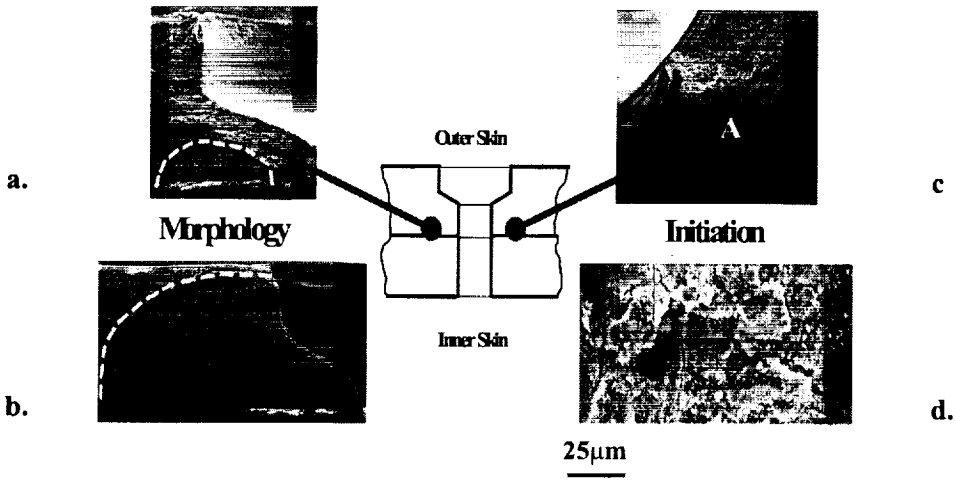

Figure 2. Counterbore rivet outer skin cracking: a) and b) SEM micrographs showing the progression of fatigue cracks (dashed lines mark the crack front), c) micrograph shows the rivet hole at an oblique angle and the location of fretting damage (region A) along the faying surface (site of crack initiation), and d) high magnification micrograph showing fretting debris and microcracks in " region A of Figure 2c".

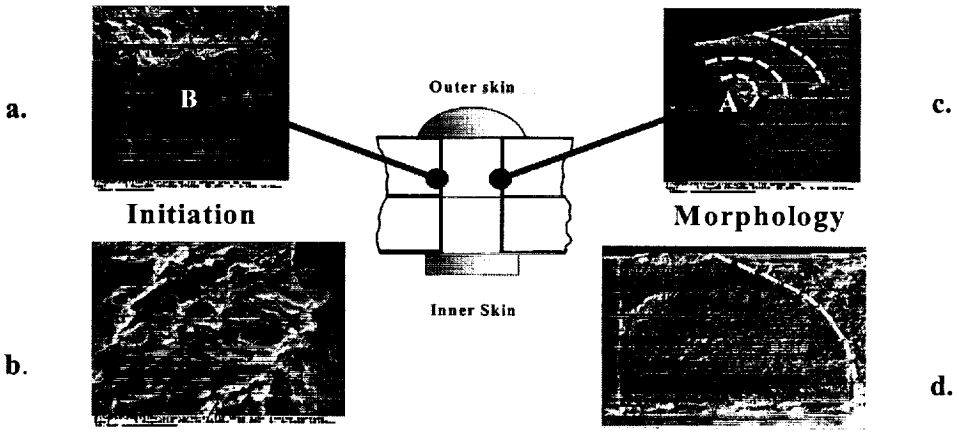

Figure 3. Straight shank rivet outer skin cracking: a) Micrograph of the crack initiation site (region A in "c"), b) high magnification micrograph of fretting surface at region B, c) the micrograph shows the region of crack initiation (region A) along the inside surface of the rivet hole near the inboard corner (dashed lines depict the progression of the fatigue crack), and d) micrograph showing a fatigue crack with multiple initiation sites (arrows) along the surface of the rivet hole (dashed line marks the crack front).

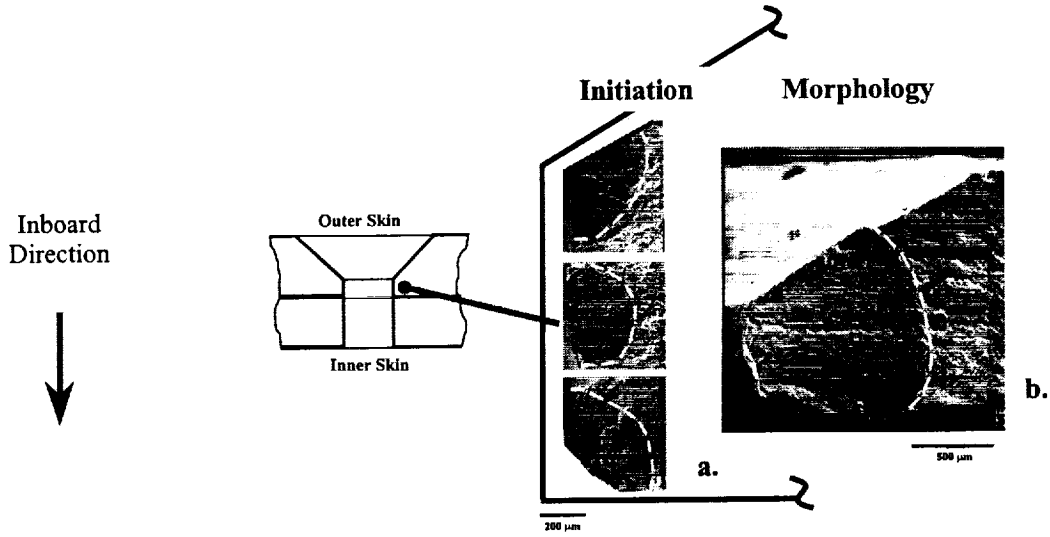

Figure 4. 100° countersink rivet outer skin fatigue cracking: a) Depicted is the outline of the rivet hole and the micrographs show the typical crack initiation sites along the rivet hole surface and crack morphology (dashed lines mark the crack front) and b) shows the typical crack front shape of a fatigue crack that has propagated nearly one-half the length of the counter sink.

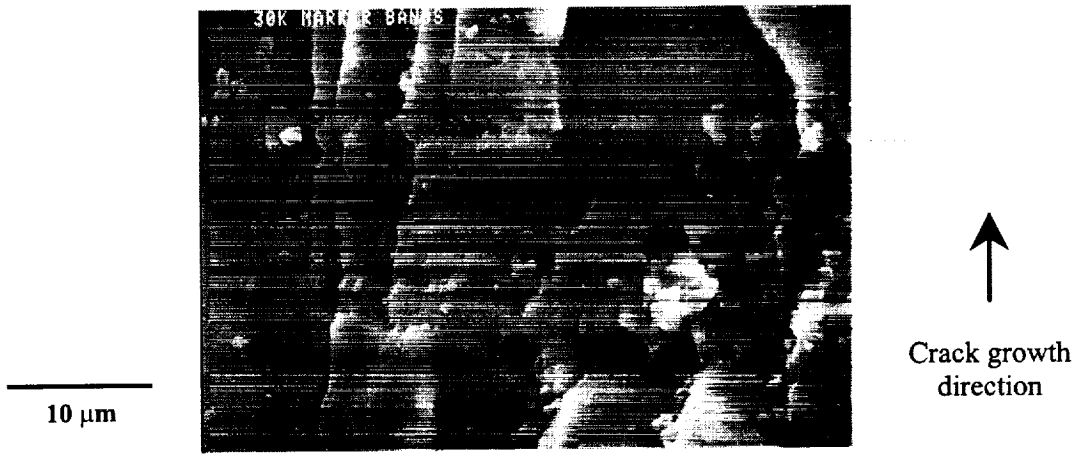

Figure 5 The micrograph shows a markerband from a fatigue crack surface in panel 1. This markerband locates the crack front at 30,000 pressure cycles.

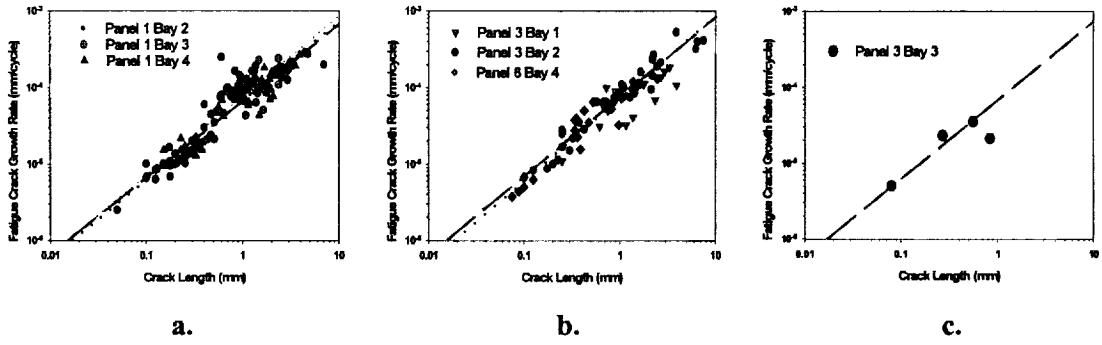

Figure 6. Plots of fatigue crack growth rate versus crack length for the a) counter bore rivet, b) straight shank rivet, and c) 100° counter sink rivet.

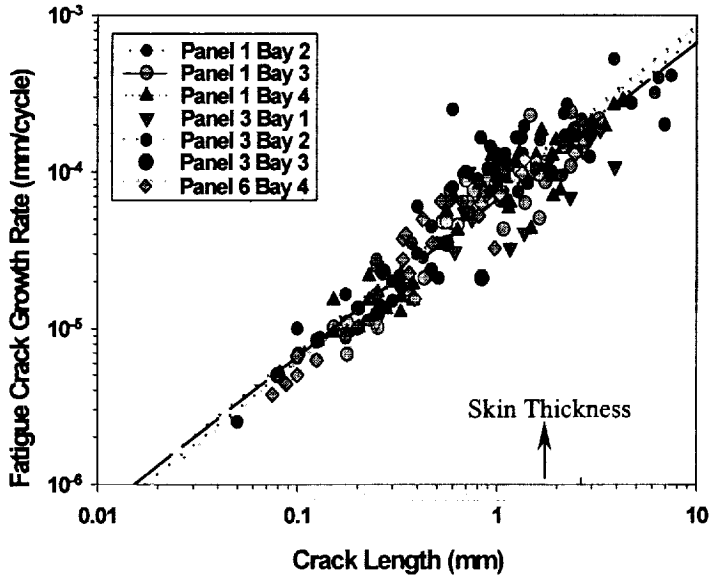

Figure 7. Summary of marker band based fatigue crack growth data from panels 1, 3, and 6.

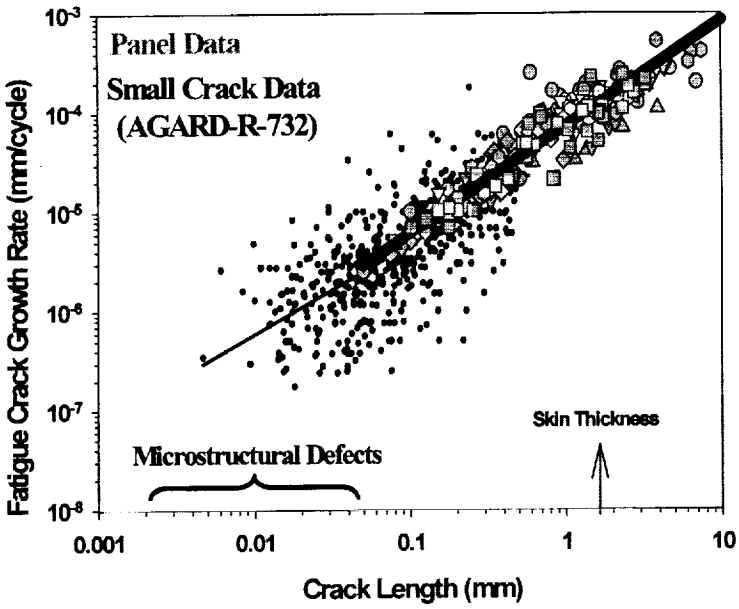

Figure 8. Comparison of small crack growth laboratory data and lap joint marker band based crack growth data from panels 1, 3, and 6.

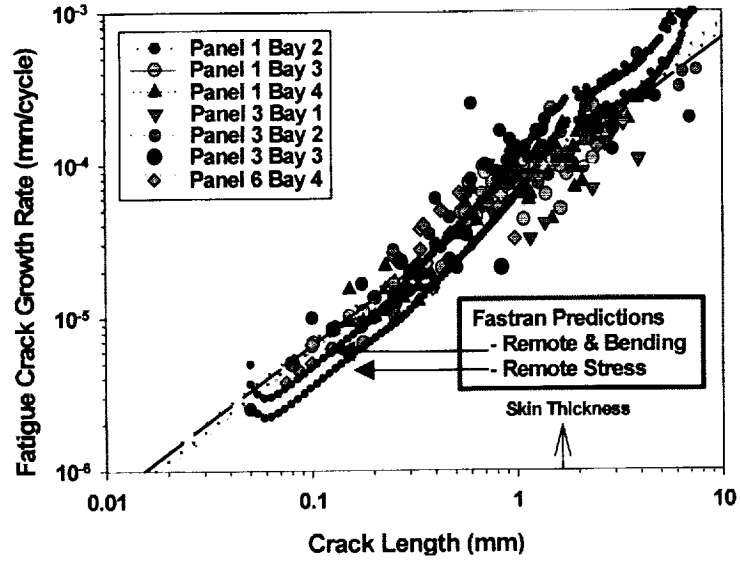

Figure 9. Comparison of two FASTRAN Code predictions (remote plus bending stress and bending stress) and crack growth rate data obtained from real aircraft lap joint structure.

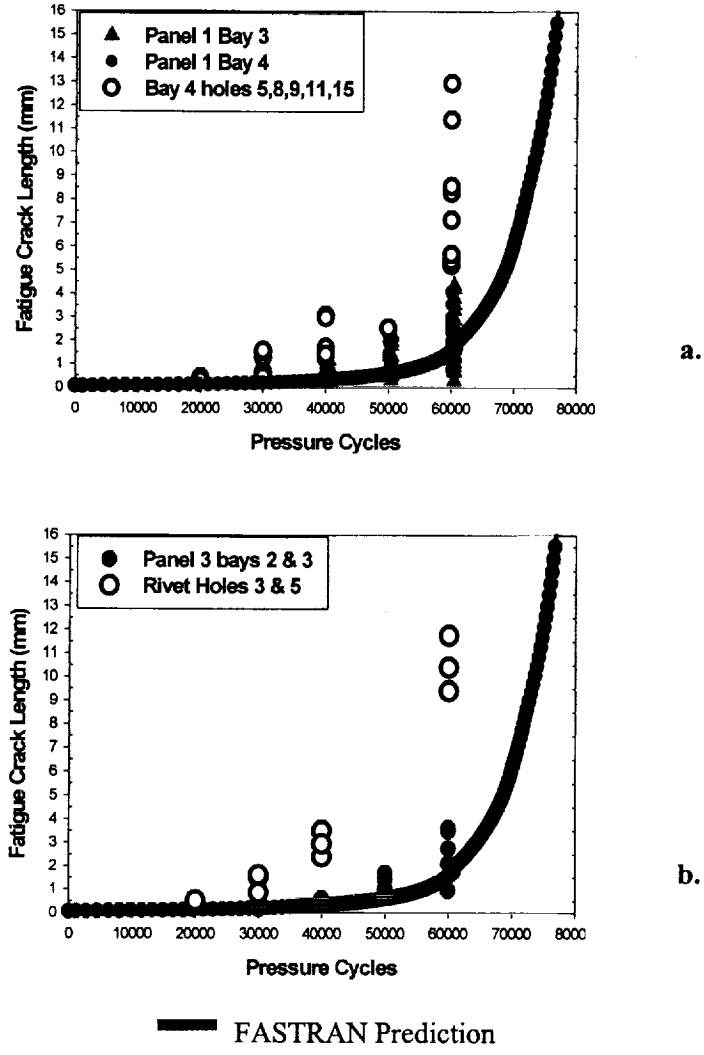

Figure 10. Comparison of FASTRAN Code prediction and marker band based crack length versus load cycle data obtained from) counterbore riveted and b) straight shank riveted structure.